This document is the Accepted Manuscript version of a Published Work that appeared in final form in Biochemistry, copyright © American Chemical Society after peer review and technical editing by publisher. To access the final edited and published work see http://dx.doi.org/10.1021/bi501353s

Dynamics of Nitric Oxide Synthase Calmodulin Interactions at Physiological Calcium Concentrations[1]

Michael Piazza, J. Guy Guillemette and Thorsten Dieckmann* [*]

Department of Chemistry, University of Waterloo, Waterloo, Ontario N2L 3G1, Canada

[1] This work was supported, in whole or in part, by the Natural Sciences and Engineering Research Council of Canada via Grants 326911 and 183521

[*] To whom correspondence should be addressed: Dept. of Chemistry, University of Waterloo, 200 University Ave. W, Waterloo, Ontario N2L 3G1 Canada. Tel. 519-888-4567 ext. 35036; Fax 519-746-0435; E-mail: tdieckma@uwaterloo.ca; jguillem@uwaterloo.ca

Abbreviations: NOS, Nitric oxide synthase; iNOS, inducible NOS; eNOS, endothelial NOS; nNOS, neuronal NOS; cNOS, constitutive NOS; CaM, Calmodulin; NMR, Nuclear magnetic resonance; CaM-iNOS, CaM-iNOS binding domain peptide; CaM-eNOS, CaM-eNOS binding domain peptide; PDB, Protein data bank; HSQC, heteronuclear single-quantum coherence; H/D, hydrogen/deuterium; cCaM, C-lobe of CaM; nCaM, N-lobe of CaM; apoCaM, Ca^{2+} deplete CaM.

ABSTRACT: The intracellular Ca^{2+} concentration is an important regulator of many cellular functions. The small acidic protein Calmodulin (CaM) serves as a Ca^{2+} sensor and control element for many enzymes. Nitric oxide synthase (NOS) is one of the proteins that is activated by CaM and plays a major role in a number of key physiological and pathological processes. Previous studies have shown CaM to act like as a switch that causes a conformational change in NOS to allow for the electron transfer between the reductase and oxygenase domains through a process that is thought to be highly dynamic. We have analyzed the structure and dynamics of complexes formed by peptides based on inducible NOS (iNOS) and endothelial NOS (eNOS) with CaM at Ca^{2+} concentrations that mimic the physiological basal (17 and 100 nM) and elevated levels (225 nM) found in mammalian cells using fluorescence techniques and NMR spectroscopy. The results show the CaM-NOS complexes have similar structures at physiological and fully saturated Ca^{2+} levels, however, their dynamics are remarkably different. At 225 nM Ca^{2+} concentrations the CaM-NOS complexes show overall an increase in backbone dynamics, when compared to the dynamics of the complexes under saturating Ca^{2+} concentrations. Specifically, the N-lobe of CaM in the CaM-iNOS complex displays lower internal mobility (higher S^2) and higher exchange protection compared to that of the CaM-eNOS complex. In contrast, the C-lobe of CaM in the CaM-eNOS complex is less dynamic. These results illustrate that structures of CaM-NOS complexes determined at saturated Ca^{2+} concentrations cannot provide a complete picture because the differences in intramolecular dynamics only become visible at physiological Ca^{2+} levels.

Calmodulin (CaM) is a small cytosolic Ca^{2+}-binding protein that is found in all eukaryotic cells. It is able to bind and regulate hundreds of different intracellular proteins.[1] CaM consists of two globular domains connected by a flexible central linker region. Each globular domain contains two EF hand pairs that are capable of binding to Ca^{2+}. Binding of Ca^{2+} to CaM causes conformational changes that expose hydrophobic patches that allow it to bind and activate its intracellular target proteins. The flexibility of CaM's central linker separating the N- and C-domains allows it to adapt its conformation to optimally associate with its intracellular targets.[2] There is considerable interest in obtaining a better understanding of the structural basis for CaM's ability to recognize, bind and regulate its numerous target proteins.

Nitric oxide synthase (NOS) enzymes (E.C. 1.14.13.39) are one of CaM's target enzymes. These enzymes catalyze the production of nitric oxide (•NO) that acts as a secondary inter- and intracellular messenger involved in many physiological processes.[3] Three NOS isozymes are found in mammals: neuronal NOS (nNOS, NOS I), endothelial NOS (eNOS, NOS III), and inducible NOS (iNOS, NOS II). NOS enzymes are homodimeric with each monomer containing an N-terminal oxygenase domain and a C-terminal reductase domain, connected by a CaM binding domain that is required for efficient electron transfer from the reductase to the oxygenase domain for •NO production. The oxygenase domain contains binding sites for the catalytic heme, tetrahydrobiopterin (H_4B), and the substrates L-arginine and molecular oxygen; the reductase domain contains binding sites for the cofactors FMN, FAD, and NADPH.[3,4] The CaM binding domains of NOS contain the classical 1-5-8-14 CaM-binding motif. CaM binds and activates the Ca^{2+}- dependent constitutive NOS (cNOS) enzymes, eNOS and nNOS, at elevated cellular Ca^{2+} concentrations.[5] In contrast, iNOS is controlled at the transcriptional level *in vivo* by cytokines and binds to CaM in a Ca^{2+}-independent manner.[6] A large conformational change that CaM induces in the reductase domain of the NOS enzymes allows for the FMN domain to interact with both the FAD and the heme to accept and pass on the electrons during catalysis.[7,8]

Understanding the structural basis of CaM's target protein interactions and diverse regulatory functions is crucial for rationalizing the regulation pathways and for developing strategies for controlling them for medical purposes. It is well established that CaM is able to interact with its target enzymes in many different conformations. CaM's interactions with the various NOS isozymes have previously been studied by NMR.[9–13] In addition to 3D structures, NMR spectroscopy can also provide quantitative information on molecular dynamics of protein systems at a residue specific level. These studies provide direct evidence of structural changes and intramolecular dynamics associated with functions that are central to understanding the role of dynamics in protein function.[14–18] By tracking chemical shift changes, NMR spectroscopy is able to characterize very weak interactions between proteins and ligands at atomic (or residue) levels.[19,20]

Detailed information about fluctuations in protein structures and site-specific information on the stability of secondary structural elements can also be obtained from the measurement of amide proton (NH) hydrogen/deuterium exchange (H/D) rates using NMR spectroscopy.[21–23] These fluctuations expose some of the NH to the D_2O solvent, thus facilitating the NH/ND exchange process while other amide protons remain protected from exchange. The exchange rate of NHs in proteins is determined by a combination of their intrinsic exchange rate in the absence of secondary structure and the presence of secondary structure and solvent inaccessibility that protect from exchange.[24,25] NH H/D exchange experiments are also useful for accessing the stability of specific structure elements within a protein or protein complex.[26,27]

Most structural and dynamics studies on CaM-NOS interactions have been performed at non-physiological conditions using either apo (Ca^{2+} free with EDTA present) or Ca^{2+} saturated (greater than 1mM Ca^{2+}) conditions. Here we present NMR structural and dynamics data of the CaM-NOS complexes at free Ca^{2+} concentrations that are in the resting intracellular Ca^{2+} concentration range of less than 100

nM,[28,29] and at elevated intracellular Ca^{2+} concentrations of 225 nM as well as under saturation conditions (1mM). Our data highlights remarkable differences in the dynamic properties of CaM-NOS complexes at high millimolar Ca^{2+} concentrations when compared to nanomolar physiological Ca^{2+} concentrations in a residue specific manner. Although the CaM-NOS complexes have similar structures at these Ca^{2+} concentrations, our studies show that the complexes behave more dynamic at lower (physiological) concentrations.

EXPERIMENTAL PROCEDURES

CaM Protein Expression and Purification. Wild-type CaM protein was expressed and purified using phenyl sepharose chromatography, as previously described.[30] Isolation of the CaM protein (148 residues) was confirmed by ESI-MS and purity was judged to be > 95% by SDS-PAGE. The human iNOS (RREIPLKVLVKAVLFACMLMRK, 22 residues corresponding to residues 510-531 from the full length iNOS protein) and eNOS (TRKKTFKEVANAVKISASLMGT, 22 residues corresponding to residues 491-512 from the full length eNOS protein) peptides were synthesized and purchased from Sigma.

Dansylation of CaM. Dansyl-CaM was prepared as previously described.[31] CaM (1 mg/ml) was buffer exchanged into 10 mM $NaHCO_3$, 1 mM EDTA, pH 10.0, at 4°C. 30 µl of 6 mM dansyl-chloride (1.5 mol/mol of CaM) in DMSO was added to 2 ml of CaM, with stirring. After incubation for 12 hr at 4°C, the mixture was first exhaustively dialyzed against 500 volumes of 150 mM NaCl, 1 mM EDTA, 20 mM Tris-HCl, pH 7.5, at 4°C, and then exhaustively dialyzed against 500 volumes of water. Labeling yields were determined from absorbance spectra using the ε_{320} of 3,400 $M^{-1}cm^{-1}$ and were compared to actual protein concentrations determined using the Bradford method with wild-type CaM used as the protein standard.[32] ESI-MS was used to confirm successful dansyl-labeling of each CaM protein. The concentration of dansyl-CaM in all experiments was 2 µM.

Steady State Fluorescence. Fluorescence emission spectra were obtained using a PTI QuantaMaster spectrofluorimeter (London,ON). Fluorescence measurements were made on 50 μL samples consisting of dansyl-CaM (2 μM) alone or with eNOS or iNOS peptide in 30 mM MOPS, 100 mM KCl, 10 mM EGTA, pH 7.2 with an increasing concentration of free Ca^{2+}. Free Ca^{2+} concentration was controlled using the suggested protocol from the calcium calibration buffer kit from Invitrogen. The excitation wavelength for all of the dansyl-CaMs was set at 340 nm and emission was monitored between 400 and 600nm. Slit widths were set at 2 nm for excitation and 1 nm for emission. Relative fluorescence was calculated by the following equation: relative fluorescence = $(F - F_0)/(F_{max} - F_0)$, where F is the measured intensity, F_{max} is the maximum intensity, and F_0 is the intensity without added Ca^{2+}.

Sample Preparation for NMR Investigation. CaM for NMR experiments was expressed in E. coli in M9 media (11.03 g/L $Na_2HPO_4 \cdot 7H_2O$, 3.0 g/L KH_2PO_4, 0.5 g/L NaCl, 2 mM $MgSO_4$, 0.1 mM $CaCl_2$, 5 mg/mL Thiamine, 100 μg/mL kanamycin) containing 2 g/L ^{13}C-glucose and 1 g/L $^{15}NH_4Cl$.[10] ^{13}C-^{15}N-CaM was purified as described above. The Ca^{2+} saturated ^{13}C-^{15}N-CaM samples were prepared for NMR experiments via a buffer exchange into 100 mM KCl, 10 mM $CaCl_2$, 0.2 mM NaN_3, 90% H_2O/10% ^2H_2O at pH 6.5 using a YM10 centrifugal filter device (Millipore Corp., Billerica, USA) and had a final concentration of 1 mM in a total volume of 500 μL. The 17 nM, 100 nM and 225 nM free [Ca^{2+}] ^{13}C-^{15}N-CaM samples were prepared via a buffer exchange into 30 mM MOPS, 100 mM KCl, 90% H_2O/10% ^2H_2O, pH 7.2, and combinations of 10 mM EGTA and 10mM CaEGTA to obtain 17 nM, 100 nM and 225 nM concentrations of free Ca^{2+}. These samples had a final ^{13}C-^{15}N-CaM concentration of 200 μM in a total volume of 500 μL. The samples were transferred into 5 mm NMR sample tubes and stored at 4°C until required for NMR experiments. NMR experiments on the complexes were conducted on samples titrated with either iNOS or eNOS peptide to saturation in a 1:1 CaM:peptide ratio. Complex formation was monitored after each addition by acquisition of a ^{1}H-^{15}N heteronuclear single-quantum

coherence (HSQC) spectrum. For the proton-deuterium exchange studies, the CaM-peptide complex samples were lyophilized overnight. The samples were then resuspended in ~100% D_2O to the same volume and immediately placed into the previously tuned and calibrated NMR spectrometer.

NMR Spectroscopy and Data Analysis. NMR spectra were recorded at 25°C on Bruker 600 MHz DRX spectrometers equipped with XYZ-gradients triple-resonance probes (Bruker, Billerica, MA, USA). Spectra were analyzed using the program CARA (Computer Aided Resonance Assignment).[33] The amide resonances were assigned by using the previously obtained amide chemical shifts of Ca^{2+} saturated CaM with iNOS or eNOS peptide as reference.[10] H/D exchange data was obtained by successive acquisition of ^{1}H-^{15}N HSQC spectra of each sample immediately after they were resuspended in D_2O. Each ^{1}H-^{15}N HSQC experiment was acquired with 32 scans and 128 increments for a total acquisition time of 100 minutes. ^{15}N T_1 measurements were acquired for eight different durations of the T_1 relaxation delay, T= 5, 100, 200, 300, 400, 500, 600, and 800ms. ^{15}N T_2 measurements were acquired for eight different durations of the T_2 relaxation delay, T= 16.6, 33.2, 49.8, 66.4, 99.6, 116.2, 132.8, and 149.4ms. ^{1}H-^{15}N NOE measurements were recorded with two spectra, one with the NOE effect and one without. The standard model free approach[34] was used to determine order parameters (S^2) for each of the CaM-peptide complexes. The order parameters were calculated using the TENSOR program (version 2.0).[35,36]

Model of CaM-eNOS Peptide at 225 nM [Ca^{2+}]. In order to visualize the dynamics data a model of CaM-eNOS peptide at 225 nM [Ca^{2+}] was prepared using CNSsolve version 1.2.[37] The calculation used the structural constraints for the C-terminal residues from the solution structure of CaM with eNOS at saturated Ca^{2+} along with the inter-residue constraints of the C-terminal residues to the eNOS peptide. All N-terminal intra and inter-residue constraints were deleted and replaced with constraints for the N-terminal residues from the apoCaM structure deposited in the PDB (1CFC). The structure calculation

was initiated with an extended conformation file. The calculation was run through several iterations of a standard simulated annealing protocol to minimize the energies. The average of the final 20 lowest energy structures was selected for the visualization model.

RESULTS

Fluorescence Spectroscopy of Dansyl-CaM Binding to NOS Peptides. The Ca^{2+} dependent binding properties of the CaM binding domains used in our study were first investigated using dansyl-labeled CaM proteins (Figure 1). Dansyl-CaM is a useful tool to detect conformational changes in CaM as a result of interactions with Ca^{2+}, peptides or other proteins because the intensity of the fluorescence spectrum is enhanced and shifted when the dansyl moiety becomes embedded in a hydrophobic environment.[31,38] Without peptides or Ca^{2+} present, dansyl-CaM exhibited a fluorescence maximum at 510nm (Figure S1a of Supporting Information). When Ca^{2+} was titrated into the sample a blue shift (to 490nm) and enhancement of dansyl fluorescence spectrum were observed in a Ca^{2+} concentration range of 0.65-2.86 μM (Figure 1).

When iNOS peptide was added in the absence of Ca^{2+} the same blue shift and enhancement of dansyl fluorescence spectrum observed with addition of Ca^{2+} to CaM alone was seen, but not when eNOS peptide was added to the dansyl-CaM (Figure S1b, c of Supporting Information). The dansyl-CaM-iNOS complex showed no Ca^{2+} dependency when Ca^{2+} was titrated into the sample, as indicated by the lack of fluorescence change (Figure S1b of Supporting Information) and little relative fluorescence difference over the whole range of free Ca^{2+} concentration additions (Figure 1). With the addition of Ca^{2+}, this blue shift and enhancement of the fluorescence spectrum seen with CaM alone was then also observed with the eNOS peptide. However, the fluorescence changes of the dansyl-CaM-eNOS complex occurred at a much lower Ca^{2+} concentration range, beginning at 225 nM. This is consistent with previous studies of eNOS that show the enzyme requires 200-300 nM concentrations of free Ca^{2+} to

achieve half maximal activity.[39,40] Hence a concentration of 225 nM free Ca^{2+} was used for the NMR studies, corresponding to physiological Ca^{2+} concentrations above basal levels.

NMR Spectroscopy at Physiological Ca^{2+} Concentrations. NMR experiments were performed at physiological free Ca^{2+} concentrations to provide further insights into the structural differences between the two CaM-NOS complexes. ^{1}H-^{15}N HSQC spectra show that the CaM-eNOS complex at a physiological free Ca^{2+} concentration of 225 nM has a C-terminal lobe that is structurally similar to the Ca^{2+}-replete CaM-eNOS complex (Figure 2a, b), and an N-terminal lobe structurally similar to unbound, Ca^{2+} free apoCaM (Figure 2c, d). This can be visualized by overlaying the ^{15}N-HSQC spectra of CaM-eNOS at 225 nM free [Ca^{2+}] with either Ca^{2+}-replete CaM-eNOS or apoCaM. Cross peaks for amides in the C-domain of CaM-eNOS at 225 nM [Ca^{2+}] overlap with those of Ca^{2+}-replete CaM-eNOS, but amides in the N-domain do not (Figure 2a). And vice versa, cross peaks for amides in the N-domain of CaM-eNOS at 225 nM [Ca^{2+}] overlap with those of apoCaM, but amides in the C-domain do not (Figure 2c). More specifically the cross peaks assigned to G25 (EF1), G61 (EF2), I27, I63 (the short antiparallel β-sheets between EF1 and EF2), G98 (EF3), G134 (EF4) and I100 and V136 (the short antiparallel β-sheets between EF3 and EF4) have specific chemical shifts characteristic of Ca^{2+} binding to each EF hand and the conformation of the EF hand pairs. The cross peaks assigned to G98, G134, I100 and V136 for CaM-eNOS at 255 nM Ca^{2+} have very similar chemical shifts to those assigned for Ca^{2+}-replete CaM-eNOS, indicating that the C-lobe of CaM at 225 nM [Ca^{2+}] is Ca^{2+} replete and bound to the eNOS peptide. On the other hand, the cross peaks assigned to G25, G61, I27 and I63 have very similar chemical shifts to those assigned for apoCaM, indicating that the N-lobe of CaM at 225 nM [Ca^{2+}] is Ca^{2+} deplete and not bound to the eNOS peptide.

This behavior is clearly shown by calculating the chemical shift difference between each set of amides. In the overlay of CaM-eNOS at 225 nM free [Ca^{2+}] and Ca^{2+}-replete CaM-eNOS the amide

chemical shifts show a difference for all the residues of the N-domain, whereas the amide chemical shifts of the C-domain have very small differences (Figure 2b). In the overlay of CaM-eNOS at 225 nM [Ca^{2+}] and apoCaM the amide chemical shifts show a difference for all the residues of the C-domain, whereas the amide chemical shifts of the N-domain have very small differences (Figure 2d). Comparison of the ^{1}H-^{15}N HSQC spectrum of the eNOS-CaM complex under Ca^{2+} replete versus that at a Ca^{2+} concentration of 225nM clearly shows that the C-lobe of CaM is the first to bind to Ca^{2+} and the eNOS peptide. This is further supported by comparing the ^{1}H-^{15}N HSQC spectra in the presence of 225nM [Ca^{2+}] and the apo form of the CaM. These results are consistent with the known Ca^{2+} binding properties of the N and C lobes of free CaM in solution.[41,42]

When a similar comparison is made using the CaM-iNOS complex, ^{1}H-^{15}N HSQC spectra indicate that the CaM-iNOS complex maintains structural integrity at all Ca^{2+} levels (Figure 3). This observation makes sense because CaM interacts with iNOS in a Ca^{2+}-independent manner. Figure 3 shows ^{1}H-^{15}N HSQC spectra of CaM-iNOS at 17 nM, 100 nM and 225 nM free [Ca^{2+}]. The spectra at all 3 of these low Ca^{2+} levels show the same chemical shift patterns for the amides (Figure 3a- c), indicating that the structure of this complex doesn't change going from free Ca^{2+} levels representative of resting intracellular Ca^{2+} levels (17 and 100 nM Ca^{2+}) to elevated Ca^{2+} levels (225 nM Ca^{2+}). When these spectra are compared to the ^{1}H-^{15}N HSQC spectrum of CaM-iNOS complex at saturated [Ca^{2+}] (10 mM Ca^{2+}) we see that the spectra all overlay quite well. The few amide cross peaks that are slightly shifted are likely due to the different buffer and pH used for the low Ca^{2+} sample (pH 7.2) and saturated Ca^{2+} samples (pH 6.5). A comparison of the specific cross peaks characteristic of Ca^{2+} binding to each EF hand and the conformation of the EF hand pairs as done with CaM-eNOS for all the CaM-iNOS samples illustrates that the structure of CaM bound to the iNOS peptide is very similar at low and high free Ca^{2+} concentrations. This suggests that the CaM-iNOS complex binds Ca^{2+} at this low basal Ca^{2+} level. NMR

data could not be collected for the iNOS peptide interacting with apoCaM or CaM_{1234} (CaM that contains a mutation in each EF hand that disables Ca^{2+} binding) due to precipitation of the protein upon addition of the peptide. This behavior has also been seen in other studies at higher concentrations of CaM and iNOS peptide.[43,44] This suggests that in the Ca^{2+} deplete form CaM-iNOS adopts a different conformation which may expose hydrophobic regions that leads to this aggregation, or that a larger portion of the iNOS enzyme is required for binding in apo conditions, as previously suggested.[40]

Amide Exchange and Internal Protein Dynamics for CaM-eNOS Complexes at Low and Saturating Ca^{2+} Concentrations. H/D exchange patterns of amides were classified into three categories based on the length of time for which the amide peaks were observable in the spectra after D_2O exposure: fast exchange (amide peaks disappear before first experiment); intermediate exchange (amide peaks disappear between 3 min and 100 min); and slow exchange (amide peaks remained longer than 200 min). The criteria for slow exchange were based on the observation that little change occurs in the spectrum when additional ^{1}H-^{15}N HSQC spectra were obtained after 200 min (data not shown). An intermediate exchange lower limit of 3 min was determined by the amount of time elapsed prior to the acquisition of the first NMR spectrum.

The amide exchange investigation of the CaM-eNOS complex under Ca^{2+} saturated conditions showed very little change over the period investigated (Figure 4a-c). Relatively few residues have undergone exchange with the D_2O as evidenced by the lack of signal disappearance in the ^{1}H-^{15}N HSQC spectra. The few residues that have undergone exchange are found to be at the N and C termini, in the loop regions between the two EF hands in each lobe of CaM and in the linker region. These are residues that are exposed to the solvent and are not well protected by secondary structure elements, such as H-bonding in α-helices, or by binding to the eNOS peptide. Figure 6a shows the H/D exchange data projected onto the previously determined structure of the Ca^{2+} replete CaM-eNOS complex.[10,45]

Residues that have undergone fast exchange were colored red, while residues that exhibit intermediate exchange have been colored light blue and residues exhibiting slow exchange colored blue.

When the same set of experiments were performed at 225 nM [Ca^{2+}], after 100 min most amide protons exchanged with the D_2O as shown by the lack of amide cross peaks in the ^{1}H-^{15}N HSQC spectrum. After 200 min only a very few amide resonances remained (Figure 4d-f). The amides that exhibited fast H/D exchange were mostly found to be from residues in the N-lobe of CaM, while those that were protected from exchange, and most of those exhibiting intermediate exchange, belonged to residues in the C-lobe of CaM. This amide H/D data was projected onto a model representative of the NMR data for the CaM-eNOS complex at 225 nM [Ca^{2+}], using the same color scheme as above, with the side chains of the slow exchanging residues shown (Figure 6b). Note that this model has been prepared to better visualize the differences between the structure of the CaM-eNOS complex at the 225 nM Ca^{2+} concentration compared to the structure at saturating Ca^{2+} concentrations. It does not represent a 3D solution structure of the complex under these conditions.

As was described above, the ^{1}H-^{15}N HSQC data suggest that only the C-lobe of CaM is found to be Ca^{2+}-replete and bound to the eNOS peptide, while the N-lobe would be Ca^{2+} free and not bound to the peptide. Since the N-lobe is not bound to the peptide it would be more exposed to the solvent, which could explain why almost all of the N-lobe residues undergo fast exchange. There are a few residues of the N-lobe that exhibit intermediate exchange, such as K30, M36, M51, M72 and M76. These residues are all part of α-helices and are found to directly interact with L509, one of the anchoring residues of eNOS, in the crystal and solution structures of the complex (Table S1 of Supporting Information).[10,45,46] This suggests that even though this lobe is Ca^{2+} free and not tightly bound to the peptide it is still maintaining its structural integrity and might also maintain some transient interactions with the peptide. The amides of the C-lobe residues that show intermediate or slow exchange have been previously shown

to interact with the 1-5-8-14 anchoring residues of the eNOS peptide.[10,45] The four slow exchanging amides correspond to residues L105, L112, E140 and F141 which interact with the anchoring residues F496, A500 and V503 of the eNOS peptide in the structure of the Ca^{2+}-replete CaM-eNOS complex. The amides that show intermediate exchange are found to either interact with these anchoring residues of the eNOS peptide or be a part of α-helices in this lobe.

The internal dynamics of the CaM complexes at 225 nM [Ca^{2+}] and saturating [Ca^{2+}] were further investigated by measuring the relaxation properties of the backbone ^{15}N nuclei in CaM. T_1, T_2, and ^1H-^{15}N NOE values were measured (Figures S2 and S3 of Supporting Information). The standard model free approach[34] was used to determine order parameters (S^2) and internal correlation times (τ_i) for each of the CaM-peptide complexes (Figures 6, S2, S3 and Table S2 of Supporting Information). The comparison of the internal dynamics between the CaM-eNOS complex at 225 nM [Ca^{2+}] and saturating [Ca^{2+}] agrees well with the results found for the H/D exchange experiments. For the CaM-eNOS complex at saturating Ca^{2+} concentration low S^2 and high τ_i values were found for the residues of the linker region and also in the loop regions between the EF hand pairs. The high degree of mobility observed in these regions agrees very nicely with the H/D exchange data, which is shown in figure 6a by the correlation between worm radius and structure color. S^2 values for the rest of CaM were between 0.8 and 1.0, indicating very little mobility, and agreeing very well with the high degree of exchange protection observed in the H/D exchange data.

When the internal dynamics were analyzed for the CaM-eNOS complex at 225 nM [Ca^{2+}], a significant increase of internal dynamics is found, especially in the N-lobe. The linker region shows the same high degree of mobility as observed at saturating [Ca^{2+}]. However, an increase of mobility is observed for the loop regions between the EF hand pairs, which can be seen by comparing figures 6a and 6b. The average order parameter values for each structural element of the C-lobe are very similar at

225 nM and saturating [Ca^{2+}] (Table S2 of Supporting Information), however, the CaM-eNOS complex at 225 nM [Ca^{2+}] displays greater fluctuation in its S^2 values, and also contains a greater number of residues that show an increased internal correlation time, τ_i (Figure S2 of Supporting Information). In contrast, the N-lobe of CaM with eNOS at 225 nM [Ca^{2+}] displays an increased internal mobility across the whole domain compared to CaM-eNOS at saturated Ca^{2+}. More specifically, EF hands 1 and 2 have average order parameter values of 0.75 and 0.72, respectively, compared to 0.92 and 0.89 for CaM-eNOS at saturating [Ca^{2+}] (Table S2 of Supporting Information). The N-terminal residues, EF hands and loop region between the EF hand pairs also show an increased τ_i compared to CaM-eNOS at saturating [Ca^{2+}], indicating faster internal motions for these regions at 225 nM [Ca^{2+}]. The observed increased mobility, shown by the lower S^2 and increased τ_i, for the N-lobe of CaM indicates a more dynamic and less rigid structure for this lobe, which correlates well with the H/D exchange data.

Amide Exchange and Internal Protein Dynamics for CaM-iNOS Complexes at Low and Saturating Ca^{2+} Concentrations. The amide exchange experiments of the CaM-iNOS complex under Ca^{2+} saturated conditions showed very little change over the time period investigated (Figure 5a-c), with the same location of residues undergoing H/D exchange as did in the CaM-eNOS complex. This H/D exchange data was projected onto the previously determined solution structure of the Ca^{2+}-replete CaM-iNOS complex[10,46] using the same color scheme as described earlier (Figure 6c). However, in contrast to the CaM-eNOS complex at 225nM Ca^{2+} concentration, the C-lobe amides of the CaM-iNOS complex at 225nM Ca^{2+} concentration had faster exchange rates than the N-terminal residues (Figure 5d-f). The amides that undergo slow and intermediate exchange correspond to residues that have been found to interact with the 1-5-8-14 anchor residues (L515, V519, V522, and L528) of the iNOS peptide (Figure 5d-f, 6d and Table S1 of Supporting Information). The iNOS peptide contains hydrophobic residues (V522, L523, Met527, and L528) that interact with hydrophobic residues of the N-lobe of CaM (F16,

F19, M36, L39, Met71, Met72, and Met76).[10,46] The slower exchange of these N-lobe CaM residues shows they are protected from the D_2O solvent, indicating this is a tight hydrophobic interaction with the iNOS peptide. In contrast to the iNOS peptide, the eNOS peptide contains hydrophilic residues at these locations (with the exception of V503 and L509) that are exposed to the solvent and do not protect the CaM from exchange as shown in the H/D exchange data. The amides of the C-lobe residues of CaM display mostly fast exchange, indicating that there is less protection due to a weaker interaction with the iNOS peptide.

Analyzing the internal dynamics between the CaM-iNOS complex at 225 nM [Ca^{2+}] and saturating [Ca^{2+}] shows them to agree well with the results found for the H/D exchange experiments. For the CaM-iNOS complex at saturating [Ca^{2+}] low S^2 and high τ_i values were found for the residues of the linker region and also in the loop regions between the EF hand pairs, much like was observed in the CaM-eNOS complex at saturating [Ca^{2+}], which agrees very nicely with the H/D exchange data, (Figure 6c). S^2 values for the rest of CaM were between 0.8 and 1.0, indicating very little mobility, and agreeing very well with the high degree of stability observed from the H/D exchange data.

When the internal dynamics were analyzed for the CaM-iNOS complex at 225 nM [Ca^{2+}], the same high degree of mobility observed for the linker region and for the loop regions between the EF hands at saturating [Ca^{2+}] is shown (Figures 6c, d). The average order parameter values for each structural element of the complex are quite similar at 225 nM and saturating [Ca^{2+}] (Table S2 of Supporting Information), however, the CaM-iNOS complex at 225 nM [Ca^{2+}] displays greater fluctuation in its S^2 values, and also contains a greater number of residues that show an increased τ_i, The observed increase in τ_i for the EF hands and loop regions of CaM indicates that the residues in these regions exhibit faster internal motions at 225 nM [Ca^{2+}] (Figure S3 of Supporting Information). Also Helix H of the CaM-iNOS complex at 225 nM [Ca^{2+}] is found to have an increased internal mobility (lower S^2 values)

compared to CaM-iNOS at saturated [Ca^{2+}]. This data indicates that the CaM-iNOS complex has increased internal mobility at lower [Ca^{2+}], with a more dynamic C-lobe than N-lobe, which correlates well with the H/D exchange data.

DISCUSSION

CaM is able to fine-tune the orientation of its domain and residue contacts to accommodate its binding to a variety of target proteins. Mammalian NOS enzymes provide an ideal system for investigating the differences in Ca^{2+} dependent activation of target enzymes. The structures of CaM interacting with target peptides derived from the three enzymes have all been shown to be very similar and to consist of two EF hand pairs lined by a short connector wrapped around a helical peptide target. However, the three NOS enzymes show different Ca^{2+} dependent activation by CaM. The iNOS enzyme is fully active at basal levels of Ca^{2+} (<100 nM) in a cell, eNOS enzymes require 200-300 nM concentrations of free Ca^{2+} to achieve half maximal activity.[39,40] Most investigations have focused on the Ca^{2+} dependent activation of NOS enzymes by CaM under non-physiological conditions. Experiments are generally performed in the presence of excess Ca^{2+} or excess Ca^{2+} chelator. In the present study, more physiological relevant free Ca^{2+} conditions were used to investigate the differential CaM Ca^{2+}-dependent binding and activation of iNOS end eNOS enzymes. The dynamics of the binding were monitored using NMR H/D exchange and ^{15}N relaxation experiments under different physiologically relevant free Ca^{2+} concentrations to provide a better understanding of the process. In addition, this approach identified the roles played by the N and C lobes of CaM in the binding and activation of the NOS enzymes. This is important since the binding of Ca^{2+} to CaM is cooperative within each lobe of CaM but not between the lobes, meaning that Ca^{2+}-binding to N- and C-domains is exclusive from one another.[41,42] On its own, the C-lobe of CaM binds Ca^{2+} with a higher affinity ($K_d = 10^{-6}M$) than the N-lobe ($K_d = 10^{-5}M$).

The Ca^{2+} titration fluorescence experiments provide information about the conformational transitions of CaM during the binding of peptides and Ca^{2+}. In the absence of peptides CaM undergoes a conformational transition from apo to Ca^{2+} bound at Ca^{2+} concentrations above 650 nM. When iNOS peptide is added to the dansyl-CaM a fluorescence maximum is seen at 490nm and no transition is observed during the Ca^{2+} titration, indicating CaM is bound to the iNOS peptide in both the absence and presence of Ca^{2+}. In contrast, the eNOS peptide is not bound to CaM in the absence of Ca^{2+} but binds to CaM when the Ca^{2+} concentration is at least 225 nM, consistent with the results reported for holo eNOS enzymes.[39,40]

At Low Ca^{2+} Concentrations CaM's N-Lobe Dissociates From the eNOS Peptide. At resting intracellular Ca^{2+} concentrations CaM is unable to bind to the eNOS CaM binding domain peptide, whereas it can bind at an elevated free Ca^{2+} concentration of 225 nM. At 225 nM free [Ca^{2+}] NMR data shows the CaM-eNOS complex displays a structure where the C-lobe is bound to the peptide, but the N-lobe is not. In a previous investigation, we used gel mobility shift assays to monitor the binding of the eNOS peptide to different truncated half CaM constructs under Ca^{2+} replete conditions.[30] No binding was observed between eNOS and nCaM, and weak binding occurred between the peptide and cCaM. These half CaMs also produced little or no activity of the eNOS enzyme. Our present results showing a closer association between the C-lobe of CaM and the eNOS peptide are consistent with our previous binding studies.

CaM-iNOS Complex Has Similar Conformations at Physiological and Saturating Ca^{2+} Levels. Most studies analyzing this Ca^{2+}-independent nature of CaM and iNOS use apoCaM, however the cellular environment is not fully deplete of Ca^{2+}, with the basal intracellular Ca^{2+} concentration being on the order of 50-100 nM.[28,29] In order to characterize the complex under these physiological conditions ^{1}H-^{15}N HSQC experiments of the CaM-iNOS complex were performed at various free Ca^{2+}

concentrations ranging from resting intracellular Ca^{2+} levels to elevated Ca^{2+} levels and compared to fully saturated Ca^{2+}-CaM conditions. The current study suggests that CaM adopts the same structure as observed in Ca^{2+}-replete CaM-iNOS when bound to the iNOS peptide at both resting and elevated intracellular Ca^{2+} levels.

Activity of the iNOS enzyme decreased to less than 25% when co-expressed with a mutant CaM_{1234} used to emulate apoCaM.[47] In a study by Ruan et al[40], iNOS was found to be maximally active at Ca^{2+} concentrations as low as 0.1 nM in vitro and thus is probably maximally active in vivo at basal intracellular Ca^{2+} levels. This suggests that at the lowest Ca^{2+} level (17 nM) used in this study the CaM-iNOS complex is Ca^{2+} replete, otherwise a decrease in iNOS activity at Ca^{2+} concentrations as low as 0.1 nM would have been seen.

CaM-eNOS and CaM-iNOS Complexes Show Different Dynamic Interactions at Low and Saturating Ca^{2+} Concentrations. The dynamic properties of these complexes were further investigated by performing amide H/D exchange time-course experiments and NMR ^{15}N relaxation experiments. NH exchange experiments provide detailed information on the degree of protection of specific residues within a protein or protein complex. This information is useful for determining the stability of secondary structural elements and also identifying residues involved in co-operative binding of a lgand.[26,48] The NMR ^{15}N relaxation experiments can be interpreted by the model-free approach to characterize backbone mobility using an order parameter S^2, which may be interpreted as the amplitude of the motion, and a correlation time, τ_i, which is the characteristic time constant of this motion.

At the 225 nM free Ca^{2+} concentration CaM alone does not bind Ca^{2+}, however, the presence of the eNOS peptide enhances the Ca^{2+} affinity of the C-lobe of CaM. The fast exchange of the C-lobe amides corresponding to the residues involved in coordinating the Ca^{2+} ions indicates that this isn't a very stable or strong interaction at the 225 nM free Ca^{2+} concentration, when compared to the strong association at

saturating [Ca^{2+}]. The few residues of the N-lobe that exhibit intermediate exchange at low [Ca^{2+}] suggest that even though this lobe is likely Ca^{2+} deplete and not bound to the peptide, based on chemical shift comparison, it still maintains its structural integrity and remains folded. This data correlates well with our previous investigation that showed only full length CaM, and not the half CaMs, is able to fully activate eNOS.[30] The internal dynamics for the CaM-eNOS complex at 225 nM [Ca^{2+}] and saturating [Ca^{2+}] also agrees with our H/D exchange data. The lower order parameters observed for the linker region and loop regions between the EF hand pairs at low and saturating [Ca^{2+}] along with the fast exchange observed from the H/D exchange data show these regions have increased internal mobility and less stability. The increased mobility, shown by the lower S^2 and increased τ_i, for the N-lobe of CaM indicates a more dynamic and less rigid structure, which correlates well with the H/D exchange data. The H/D exchange and internal mobility results show that the residues of CaM interacting with eNOS' 1-5-8-14 anchoring residues have a strong interaction at low Ca^{2+} concentrations, which keeps the complex bound, while the rest of the residues of the CaM protein are able to fluctuate or "breathe". More specifically, the residues of the C-lobe have a lower degree of internal mobility (higher S^2) and higher exchange protection, indicating stronger interaction with the eNOS peptide to hold the complex together, while the N-lobe is more dynamic. At saturating Ca^{2+} concentrations the entire CaM-eNOS complex has become more rigid, or structurally stable, than it is at physiological Ca^{2+} levels.

In contrast, for the CaM-iNOS peptide complex at the 225 nM free Ca^{2+} concentration, the C-lobe shows faster exchange rates than the N-lobe of CaM. This supports our earlier studies using peptides bound to mutant half-CaM proteins indicating that the N-lobe of CaM may not fully dissociated from the iNOS peptide even at very low Ca^{2+} concentrations.[30] Notably when compared to Ca^{2+}-replete CaM co-expression, iNOS showed significant 70% activity when co-expressed with only nCaM and only 12% activity when co-expressed with cCaM. These results show that the N-terminal domain of CaM contains

important binding and activating elements for iNOS.[30,49] The internal dynamics for the CaM-iNOS complex also agrees with our H/D exchange data. As seen with the CaM-eNOS complex, the fast amide exchange and faster internal motions observed for the EF hands and loop regions of CaM at the 225 nM [Ca^{2+}] indicates that the co-ordination of Ca^{2+} by these residues isn't a very strong interaction when compared to saturating [Ca^{2+}]. The H/D exchange and internal mobility results show that the residues of CaM interacting with iNOS' 1-5-8-14 anchoring residues have a strong interaction at low [Ca^{2+}], while the rest of the residues of CaM display more dynamics and have less exchange protection. More specifically residues of CaM's N-lobe have a lower degree of internal mobility and higher exchange protection, indicating stronger interaction with the iNOS peptide, compared to the C-lobe. Taken together, this data indicates that the CaM-iNOS complex has increased internal mobility at lower [Ca^{2+}], with a more dynamic C-lobe than N-lobe.

At Low Ca^{2+} Concentrations CaM Has a Different Interaction With the eNOS and iNOS Peptides. Our H/D exchange and internal dynamics data show the CaM-iNOS and CaM-eNOS complexes exhibit similar dynamic differences between 225 nM and saturated [Ca^{2+}], however, the interaction with the peptide is different with respect to the individual CaM lobes at low [Ca^{2+}]. This is clearly shown by the lower degree of internal mobility (higher S^2 and less residues with τ_i values) and higher exchange protection of the residues of the N-lobe of CaM in the CaM-iNOS complex compared to those of the CaM-eNOS complex, while the residues of the C-lobe of CaM in the CaM-eNOS complex display lower internal mobility (higher S^2 and less residues with τ_i values) and higher exchange protection. Our results provide further evidence of stronger interactions of the N-lobe of CaM with the iNOS peptide compared to the eNOS peptide, contributing to the stronger binding of CaM with iNOS, as seen in previous studies.[10,46,50]

This is the first study to present NMR structural and dynamics data of the CaM-NOS complexes at free Ca^{2+} concentrations that are in the resting and elevated intracellular Ca^{2+} concentration range. These results demonstrate the importance of performing experiments on CaM-NOS interactions at Ca^{2+} concentrations that correspond to Ca^{2+} levels relevant to the regulation of NOS by CaM *in vivo*. We show that when experiments are performed at Ca^{2+} concentrations that are typically used in the literature, i.e. saturating [Ca^{2+}], the CaM-NOS systems are less dynamic than at Ca^{2+} concentrations corresponding to basal and elevated cellular levels. The studies of the CaM-NOS complexes that were carried out at saturated Ca^{2+} concentrations miss differences in dynamics that are only detectable at physiological Ca^{2+} levels. Thus, studies involving CaM interactions with NOS at saturating Ca^{2+} concentrations don't allow the investigator to see the contributions of the dynamics present in the CaM-NOS complexes. The structures at saturating Ca^{2+} concentrations don't tell the whole story, one needs to look at the dynamics at the same time to obtain a complete picture of the molecular basis of NOS regulation by CaM. This illustrates the importance of analyzing these complexes at Ca^{2+} concentrations that are within the physiological range in order to fully understand how NOS is regulated by CaM interactions *in vivo*.

ACKNOWLEDGEMENTS Molecular graphics images were produced using the UCSF Chimera package from the Resource for Biocomputing, Visualization, and Informatics at the University of California, San Francisco.

ASSOCIATED CONTENT

Supporting Information Available

Table of CaM sidechain interactions with NOS peptides; Table of average S^2 order parameter for each structure element of the CaM-NOS complexes; Figure of fluorescence emission spectra of dansyl-CaM proteins with NOS peptides; Figure of ^{15}N relaxation data and model free order parameters for the CaM-

eNOS complex at 225nM Ca^{2+} and saturating Ca^{2+} conditions; Figure of ^{15}N relaxation data and model free order parameters for the CaM-iNOS complex at 225nM Ca^{2+} and saturating Ca^{2+} conditions. This material is available free of charge via the Internet at http://pubs.acs.org.

REFERENCES

(1) Ikura, M., and Ames, J. B. (2006) Genetic polymorphism and protein conformational plasticity in the calmodulin superfamily: two ways to promote multifunctionality. *Proc. Natl. Acad. Sci. U. S. A. 103*, 1159–1164.

(2) Persechini, A., and Kretsinger, R. H. (1988) The central helix of calmodulin functions as a flexible tether. *J. Biol. Chem. 263*, 12175–12178.

(3) Alderton, W. K., Cooper, C. E., and Knowles, R. G. (2001) Nitric oxide synthases: structure, function and inhibition. *Biochem. J. 357*, 593–615.

(4) Daff, S. (2010) NO synthase: structures and mechanisms. *Nitric Oxide 23*, 1–11.

(5) Busse, R., and Mulsch, A. (1990) Calcium-dependent nitric oxide synthesis in endothelial cytosol is mediated by calmodulin. *FEBS Lett. 265*, 133–136.

(6) Balligand, J.-L., Ungureanu-Longrois, D., Simmons, W. W., Pimental, D., Malinski, T. A., Kapturczak, M., Taha, Z., Lowenstein, C. J., Davidoff, A. J., Kelly, R. A., Smith, T. W., and Michel, T. (1994) Cytokine-inducible nitric oxide synthase (iNOS) expression in cardiac myocytes. Characterization and regulation of iNOS expression and detection of iNOS activity in single cardiac myocytes in vitro. *J Biol Chem 269*, 27580–27588.

(7) Ghosh, D. K., and Salerno, J. C. (2003) Nitric Oxide Synthases: Domain structure and alignment in enzyme function and control. *Front. Biosci.* D193–D209.

(8) Welland, A., and Daff, S. (2010) Conformation-dependent hydride transfer in neuronal nitric oxide synthase reductase domain. *FEBS J. 277*, 3833–3843.

(9) Matsubara, M., Hayashi, N., Titani, K., and Taniguchi, H. (1997) Circular dichroism and ^{1}H NMR studies on the structures of peptides derived from the calmodulin-binding domains of inducible and endothelial nitric-oxide synthase in solution and in complex with calmodulin. Nascent alpha-helical structures are stabilized. *J. Biol. Chem. 272*, 23050–23056.

(10) Piazza, M., Futrega, K., Spratt, D. E., Dieckmann, T., and Guillemette, J. G. (2012) Structure and Dynamics of Calmodulin (CaM) Bound to Nitric Oxide Synthase Peptides: Effects of a Phosphomimetic CaM Mutation. *Biochemistry 51*, 3651–3661.

(11) Piazza, M., Taiakina, V., Guillemette, S. R., Guillemette, J. G., and Dieckmann, T. (2014) Solution structure of calmodulin bound to the target Peptide of endothelial nitric oxide synthase phosphorylated at thr495. *Biochemistry 53*, 1241–1249.

(12) Zhang, M., and Vogel, H. J. (1994) Characterization of the Calmodulin-binding Domain of Rat Cerebellar Nitric Oxide Synthase. *J. Biol. Chem. 269*, 981–985.

(13) Zhang, M., Yuan, T., Aramini, J. M., and Vogel, H. J. (1995) Interaction of Calmodulin with Its Binding Domain of Rat Cerebellar Nitric Oxide Synthase: A Multinuclear NMR Study. *J. Biol. Chem. 270*, 20901–20907.

(14) Kwan, A. H., Mobli, M., Gooley, P. R., King, G. F., and Mackay, J. P. (2011) Macromolecular NMR spectroscopy for the non-spectroscopist. *FEBS J. 278*, 687–703.

(15) Ishima, R., and Torchia, D. A. (2000) Protein dynamics from NMR. *Nat. Struct. Biol. 7*, 740–743.

(16) Kay, L. E. (1998) Protein dynamics from NMR. *Biochem. Cell Biol. 76*, 145–152.

(17) Kempf, J. G., and Loria, J. P. (2003) Protein dynamics from solution NMR: theory and applications. *Cell Biochem. Biophys. 37*, 187–211.

(18) Wand, A. J. (2001) Dynamic activation of protein function: a view emerging from NMR spectroscopy. *Nat. Struct. Biol. 8*, 926–931.

(19) Pochapsky, T. C., Kazanis, S., and Dang, M. (2010) Conformational plasticity and structure/function relationships in cytochromes P450. *Antioxid. Redox Signal. 13*, 1273–1296.

(20) Sikic, K., Tomic, S., and Carugo, O. (2010) Systematic comparison of crystal and NMR protein structures deposited in the protein data bank. *Open Biochem. J. 4*, 83–95.

(21) Ma, B., and Nussinov, R. (2011) Polymorphic triple beta-sheet structures contribute to amide hydrogen/deuterium (H/D) exchange protection in the Alzheimer amyloid beta42 peptide. *J. Biol. Chem. 286*, 34244–34253.

(22) Andrec, M., Hill, R. B., and Prestegard, J. H. (1995) Amide exchange rates in Escherichia coli acyl carrier protein: correlation with protein structure and dynamics. *Protein Sci. 4*, 983–993.

(23) Polshakov, V. I., Birdsall, B., and Feeney, J. (2006) Effects of co-operative ligand binding on protein amide NH hydrogen exchange. *J. Mol. Biol. 356*, 886–903.

(24) Englander, S. W., and Mayne, L. (1992) Using Hydrogen-Exchange Labeling And Two - Dimensional Nmr. *Annu. Rev. Biophys. Biomol. Struct. 21*, 243–265.

(25) Englander, S., and Kallenbach, N. (1983) Hydrogen exchange and structural dynamics of proteins and nucleic acids. *Q Rev Biophys 16*, 521–655.

(26) Williams, D. H., Stephens, E., O'Brien, D. P., and Zhou, M. (2004) Understanding noncovalent interactions: ligand binding energy and catalytic efficiency from ligand-induced reductions in motion within receptors and enzymes. *Angew. Chem. Int. Ed. Engl. 43*, 6596–6616.

(27) Williams, D. H., Stephens, E., and Zhou, M. (2003) Ligand Binding Energy and Catalytic Efficiency from Improved Packing within Receptors and Enzymes. *J. Mol. Biol. 329*, 389–399.

(28) Islam, S. (2012) Calcium Signaling, p 1267. Spinger.

(29) Carajoli, E. (1987) Intracellular Calcium Homeostasis. *Annu. Rev. Biochem. 56*, 395–433.

(30) Spratt, D. E., Newman, E., Mosher, J., Ghosh, D. K., Salerno, J. C., and Guillemette, J. G. (2006) Binding and activation of nitric oxide synthase isozymes by calmodulin EF hand pairs. *FEBS J. 273*, 1759–1771.

(31) Kincaid, R. L., Vaughan, M., Osborne, J. C., and Tkachuk, V. A. (1982) Ca^{2+}-dependent interaction of 5-dimethylaminonaphthalene-1-sulfonyl-calmodulin with cyclic nucleotide phosphodiesterase, calcineurin, and troponin I. *J. Biol. Chem. 257*, 10638–10643.

(32) Chen, R. F. (1968) Dansyl Labeled Proteins: Determination of Extinction Coefficient and Number of Bound Residues with Radioactive Dansyl Chloride. *Anal. Biochem. 25*, 412–416.

(33) Keller, R. L. J. (2005) Optimizing the Process of Nuclear Magnetic Resonance Spectrum Analysis and Computer Aided Resonance Assignment. Swiss Federal Institute of Technology, Zurich.

(34) Lipari, G., and Szabo, A. (1982) Model-Free Approach to the Interpretation of Nuclear Magnetic Resonance Relaxation in Macromolecules. 1. Theory and Range of Validity. *J. Am. Chem. Soc. 104*, 4546–4559.

(35) Dosset, P., Hus, J. C., Blackledge, M., and Marion, D. (2000) Efficient analysis of macromolecular rotational diffusion from heteronuclear relaxation data. *J. Biomol. NMR 16*, 23–28.

(36) Tsan, P., Hus, J. C., Caffrey, M., Marion, D., and Blackledge, M. (2000) Rotational diffusion anisotropy and local backbone dynamics of carbon monoxide-bound Rhodobacter capsulatus cytochrome c. *J. Am. Chem. Soc. 122*, 5603–5612.

(37) Brunger, A. T., Adams, P. D., Clore, G. M., Delano, W. L., Gros, P., Grosse-kunstleve, R. W., Jiang, J., Kuszewski, J., Nilges, M., Pannu, N. S., Read, R. J., Rice, L. M., Simonson, T., and Gregory, L. (1998) Crystallography & NMR System : A New Software Suite for Macromolecular Structure Determination. *Acta Cryst. D54*, 905–921.

(38) Johnson, J. D., and Wittenauer, L. A. (1983) A fluorescent calmodulin that reports the binding of hydrophobic inhibitory ligands. *Biochem. J. 211*, 473–479.

(39) Sessas, W. C., Harrison, J. K., Barber, C. M., Zengs, D., Durieuxn, M. E., Angelo, D. D. D., and Lynchsll, K. R. (1992) Molecular Cloning and Expression of a cDNA Encoding Endothelial Cell Nitric Oxide Synthase. *J. Biol. Chem. 267*, 15274–15276.

(40) Ruan, J., Xie, Q. W., Hutchinson, N., Cho, H., Wolfe, G. C., and Nathan, C. (1996) Inducible nitric oxide synthase requires both the canonical calmodulin-binding domain and additional sequences in order to bind calmodulin and produce nitric oxide in the absence of free Ca^{2+}. *J. Biol. Chem. 271*, 22679–22686.

(41) Linse, S., Helmersson, A., and Forsen, S. (1991) Calcium Binding to Calmodulin and Its Globular Domains. *J. Biol. Chem. 266*, 8050–8054.

(42) Pedigo, S., and Shea, M. A. (1995) Discontinuous Equilibrium Titrations of Cooperative Calcium Binding to Calmodulin Monitored by 1-D 1H-Nuclear Magnetic Resonance Spectroscopy. *Biochemistry 34*, 10676–10689.

(43) Anagli, J., Hofmann, F., Quadroni, M., Vorherr, T., and Carafoli, E. (1995) The calmodulin-binding domain of the inducible (macrophage) nitric oxide synthase. *Eur. J. Biochem. 233*, 701–708.

(44) Censarek, P., Beyermann, M., and Koch, K.-W. (2004) Thermodynamics of apocalmodulin and nitric oxide synthase II peptide interaction. *FEBS Lett. 577*, 465–468.

(45) Aoyagi, M., Arvai, A. S., Tainer, J. A., and Getzoff, E. D. (2003) Structural basis for endothelial nitric oxide synthase binding to calmodulin. *EMBO J. 22*, 766–775.

(46) Xia, C., Misra, I., Iyanagi, T., and Kim, J.-J. P. (2009) Regulation of interdomain interactions by calmodulin in inducible nitric-oxide synthase. *J. Biol. Chem. 284*, 30708–30717.

(47) Spratt, D. E., Taiakina, V., and Guillemette, J. G. (2007) Calcium-deficient calmodulin binding and activation of neuronal and inducible nitric oxide synthases. *Biochim. Biophys. Acta 1774*, 1351–1358.

(48) Pervushin, K., Vamvaca, K., Vögeli, B., and Hilvert, D. (2007) Structure and dynamics of a molten globular enzyme. *Nat. Struct. Mol. Biol. 14*, 1202–1206.

(49) Spratt, D. E., Duangkham, Y., Taiakina, V., and Guillemette, J. G. (2011) Mapping the Binding and Calmodulin-Dependent Activation of Nitric Oxide Synthase Isozymes. *Open Nitric Oxide J. 3*, 16–24.

(50) Venema, R. C., Sayegh, H. S., Kent, J. D., and Harrison, D. G. (1996) Identification, characterization, and comparison of the calmodulin-binding domains of the endothelial and inducible nitric oxide synthases. *J. Biol. Chem. 271*, 6435–6440.

FIGURE CAPTIONS

FIGURE 1**.** Ca^{2+} dependency of dansyl-CaM fluorescence with or without eNOS and iNOS peptides. Normalized fluorescence is shown for CaM, CM-eNOS complex, and CaM-iNOS complex.

FIGURE 2**.** (a) Overlay of ^{1}H-^{15}N HSQC spectra of CaM-eNOS peptide complex at 10mM $CaCl_2$ (green) and 225 nM free [Ca^{2+}] (red). (b) Chemical shift differences between CaM-eNOS peptide complex at 10mM $CaCl_2$ and 225 nM free [Ca^{2+}]. (c) Overlay of ^{1}H-^{15}N HSQC spectra of apoCaM (green) and CaM-eNOS peptide complex at 225nM free [Ca^{2+}] (red). (d) Chemical shift differences between apoCaM and CaM-eNOS peptide complex at 225nM free [Ca^{2+}].

FIGURE 3**.** (a,b,c) ^{1}H-^{15}N HSQC spectra of CaM-iNOS peptide complex at 17 nM, 100 nM and 225 nM free [Ca^{2+}]. The spectra at all 3 of these low [Ca^{2+}] levels show the same amide chemical shift patterns. (d) Overlay of ^{1}H-^{15}N HSQC spectra of CaM-iNOS peptide complex at 10mM $CaCl_2$ (green) and 225nM free [Ca^{2+}] (red). The ^{1}H-^{15}N HSQC spectra indicate that CaM-iNOS peptide complex maintains structural integrity at all Ca^{2+} levels.

FIGURE 4**.** Selected spectra from the amide H_2O/D_2O exchange time-course. (a) ^{1}H-^{15}N HSQC spectrum of CaM-eNOS peptide complex at 10mM $CaCl_2$ obtained in H_2O. The amide peaks labeled in black indicate amides that have undergone fast exchange with D_2O, amide peaks labeled grey indicate amides that have undergone intermediate exchange. (b,c) Spectra obtained 100 and 200 min after addition of D_2O. (d) ^{1}H-^{15}N HSQC spectrum of CaM-eNOS peptide complex at 225nM free [Ca^{2+}] obtained in H_2O. (e,f) Spectra obtained 100 and 200 min after addition of D_2O.

FIGURE 5. Selected spectra from the amide H_2O/D_2O exchange time-course. (a) ^{1}H-^{15}N HSQC spectrum of CaM-iNOS peptide complex at 10mM $CaCl_2$ obtained in H_2O. The amide peaks labeled in black indicate amides that have undergone fast exchange with D_2O, amide peaks labeled grey indicate amides that have undergone intermediate exchange. (b,c) Spectra obtained 100 and 200 min after

addition of D_2O. (d) ^{1}H-^{15}N HSQC spectrum of CaM-iNOS peptide complex at 225nM free [Ca^{2+}] obtained in H_2O. (e,f) Spectra obtained 100 and 200 min after addition of D_2O.

FIGURE 6.Worm models of CaM-eNOS peptide and CaM-iNOS peptide complexes at 225 nM [Ca^{2+}] and saturated [Ca^{2+}] illustrating their internal dynamics and amide H_2O/D_2O exchange data. The worm models were prepared using UCSF Chimera with the render by attribute function. The worm radius ranges from 0.25, corresponding to a S^2 value of 1, to 4, corresponding to a S^2 value of 0.4. The color of the residue represents its amide H_2O/D_2O exchange data. Residues that display fast D_2O exchange rates are colored red on the ribbon structure. Residues that display intermediate D_2O exchange rates are colored light blue on the ribbon structure. Residues that display slow D_2O exchange rates are colored blue on the ribbon structure with their side chain atoms shown. (a) Worm models and amide H_2O/D_2O exchange data for CaM-eNOS complex at 10mM $CaCl_2$ projected onto previously determined solution structure of Ca^{2+}-replete CaM-eNOS (PDB 2LL7). (b) Worm models and amide H_2O/D_2O exchange data for CaM-eNOS complex at 225nM free [Ca^{2+}] projected onto a model representative of the NMR data for the CaM-eNOS complex at 225 nM [Ca^{2+}]. (c) Worm models and amide H_2O/D_2O exchange data for CaM-iNOS complex at 10mM $CaCl_2$ projected onto previously determined structure of Ca^{2+}-replete CaM-iNOS (PDB 2LL6). (d) Worm models and amide H_2O/D_2O exchange data for CaM-iNOS complex at 225nM free [Ca^{2+}] projected onto previously determined structure of Ca^{2+}-replete CaM-iNOS (PDB 2LL6). The bound peptide is colored black and shown in wire form. The CaM-peptide complexes are viewed along the bound peptide helix from its C-terminus (front view) in the left column and rotated 90° around the horizontal axis with the C-terminus of the bound peptide on the top (side view) in the right column.

FIGURES

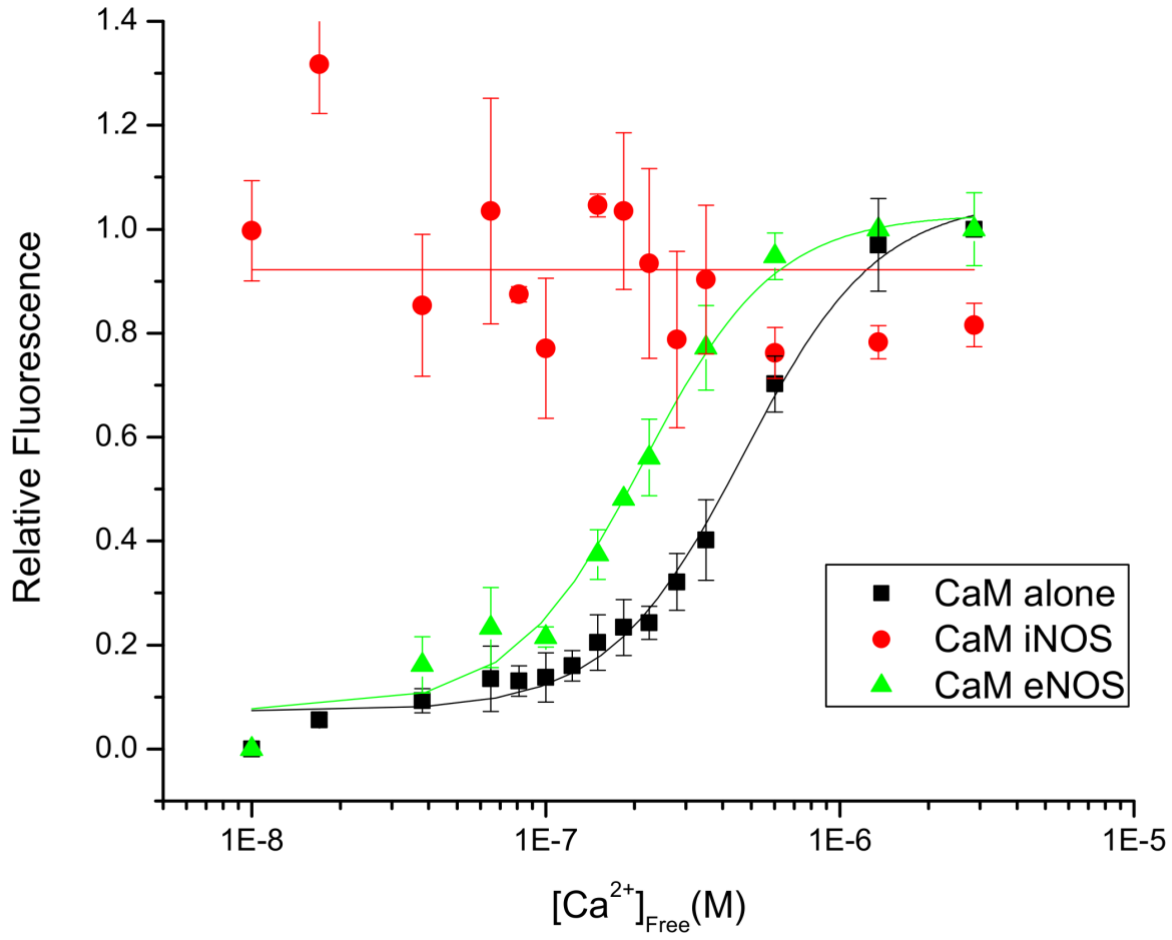

Figure 1

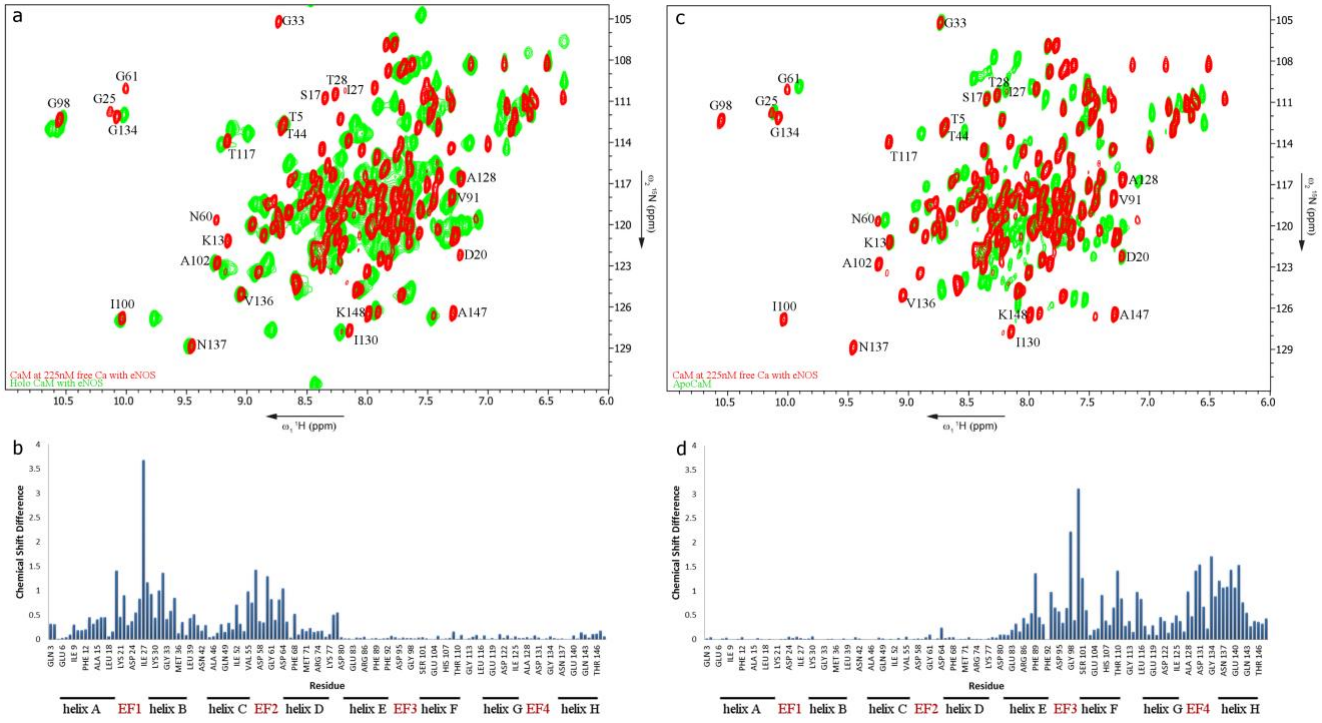
a
c
b
d
CaM at 225nM free Ca with eNOS
Holo CaM with eNOS
ApoCaM
Chemical Shift Difference
Residue
helix A
EF1
helix B
helix C
EF2
helix D
helix E
EF3
helix F
helix G
EF4
helix H

Figure 2

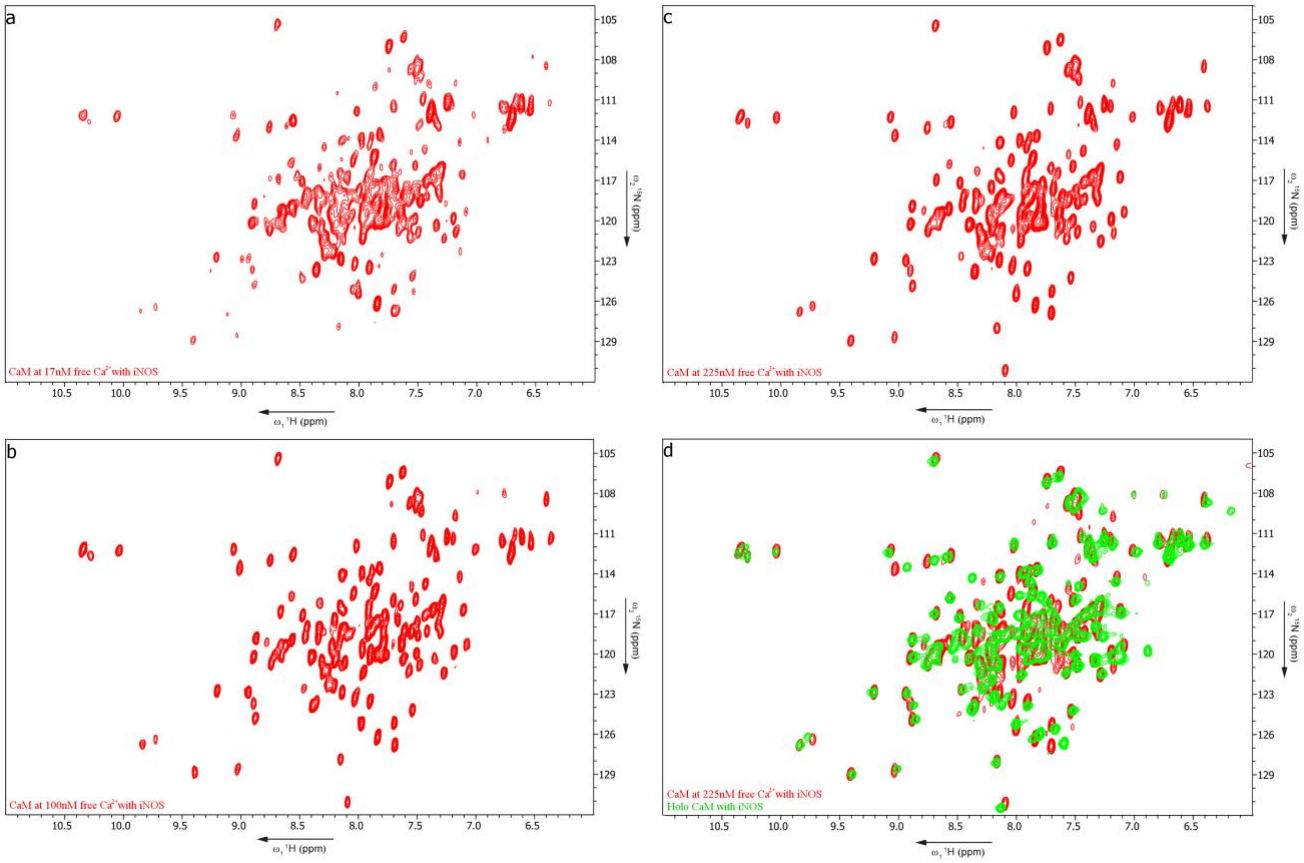
a
CaM at 17nM free Ca2+ with iNOS
b
CaM at 100nM free Ca2+ with iNOS
c
CaM at 225nM free Ca2+ with iNOS
d
CaM at 225nM free Ca2+ with iNOS
Holo CaM with iNOS
ω1 15N (ppm)
ω2 1H (ppm)

Figure 3

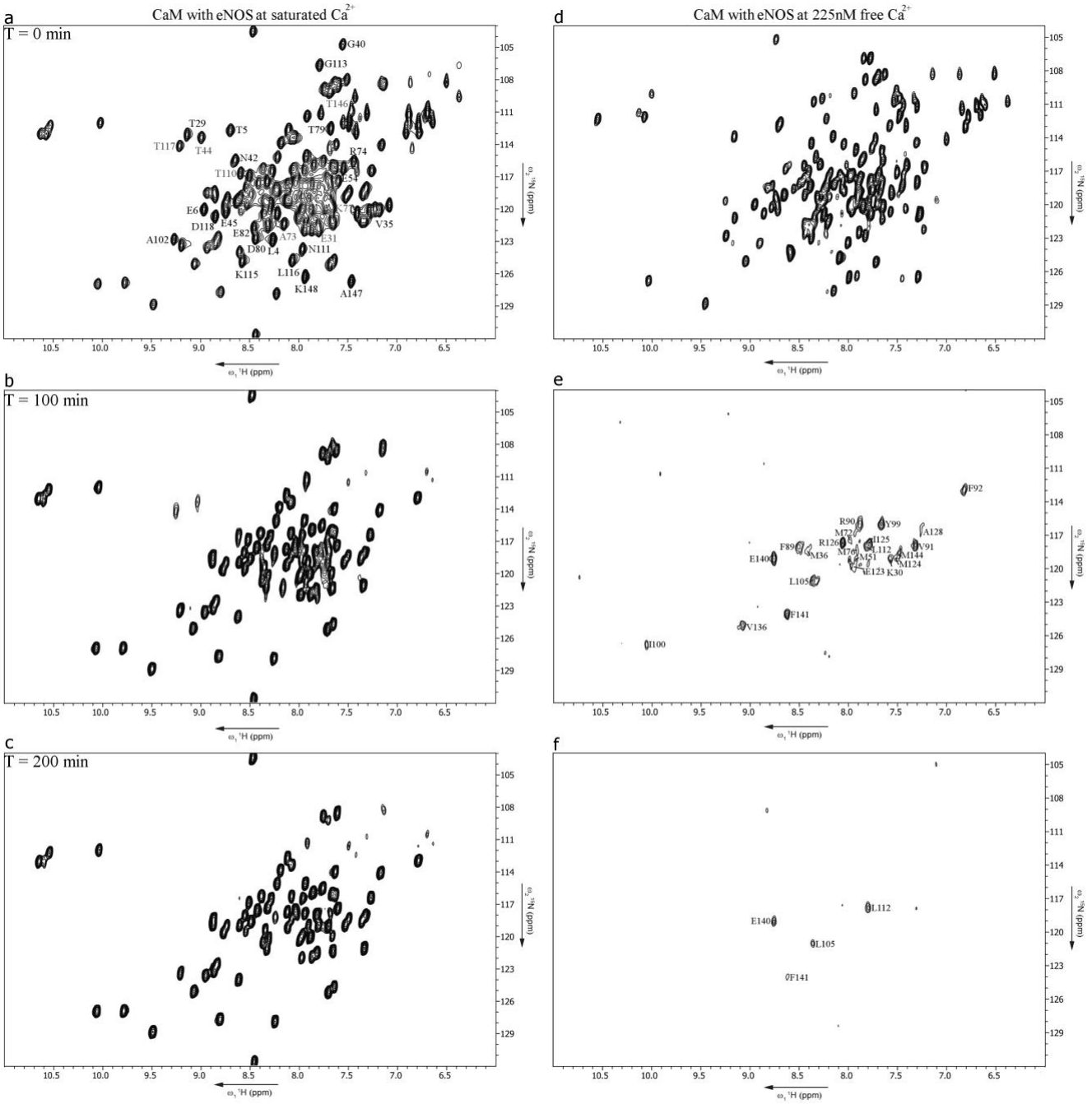
a
CaM with eNOS at saturated Ca2+
T = 0 min
G40
G113
T146
T29
T5
T79
T117
T44
R74
N42
T110
E6
D118
E45
E82
A102
D80
L4
A73
E31
N111
V35
K115
L116
K148
A147
d
CaM with eNOS at 225nM free Ca2+
b
T = 100 min
e
F92
R90
Y99
A128
M72
I125
R126
F89
M36
I112
V91
M76
M51
M144
M124
E140
E123
K30
L105
F141
V136
I100
c
T = 200 min
f
L112
E140
L105
F141
ω1 1H (ppm)
ω2 15N (ppm)

Figure 4

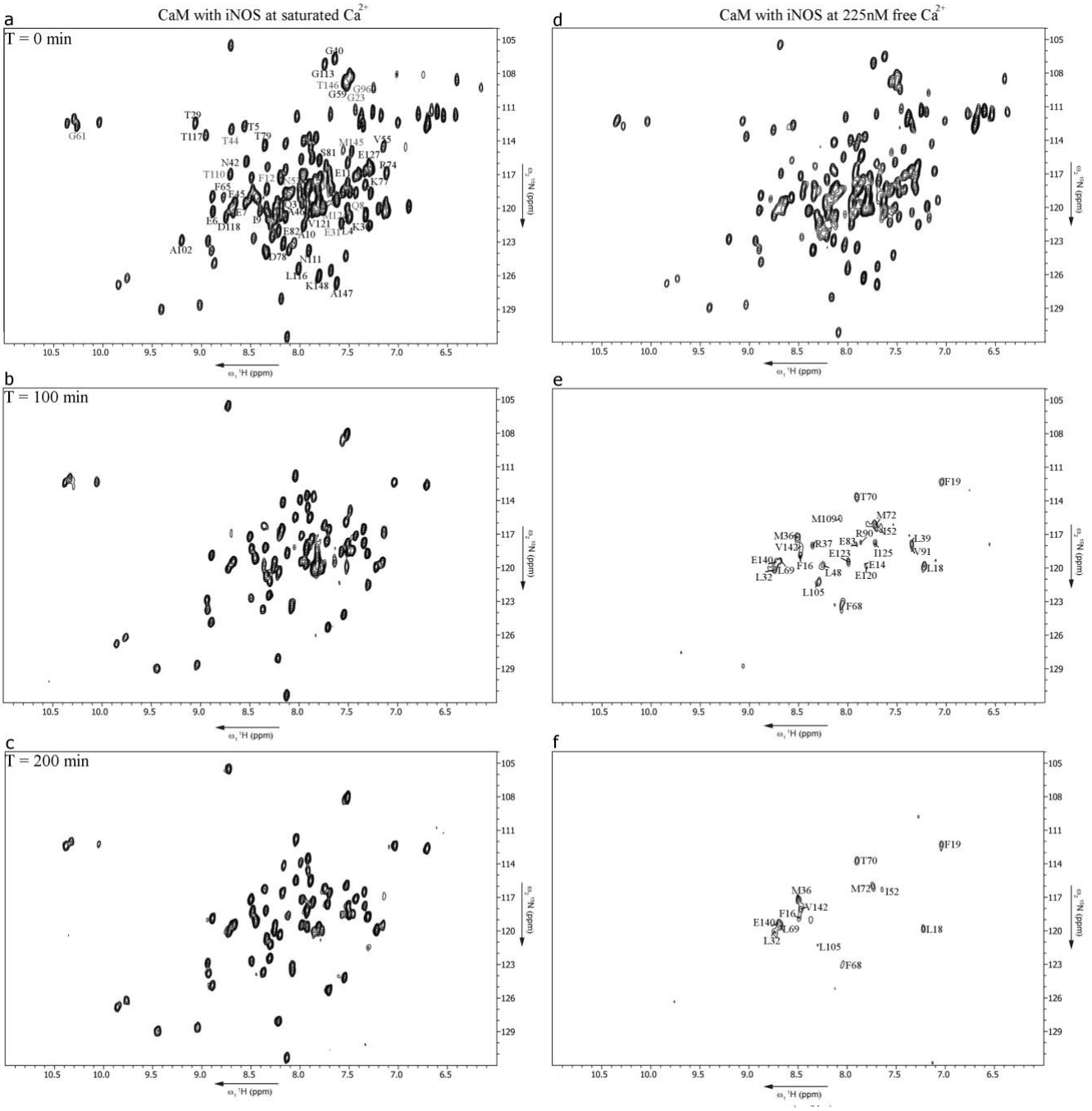
a
CaM with iNOS at saturated Ca2+
T = 0 min
b
T = 100 min
c
T = 200 min
d
CaM with iNOS at 225nM free Ca2+
e
f
ω2 15N (ppm)
ω1 1H (ppm)

Figure 5

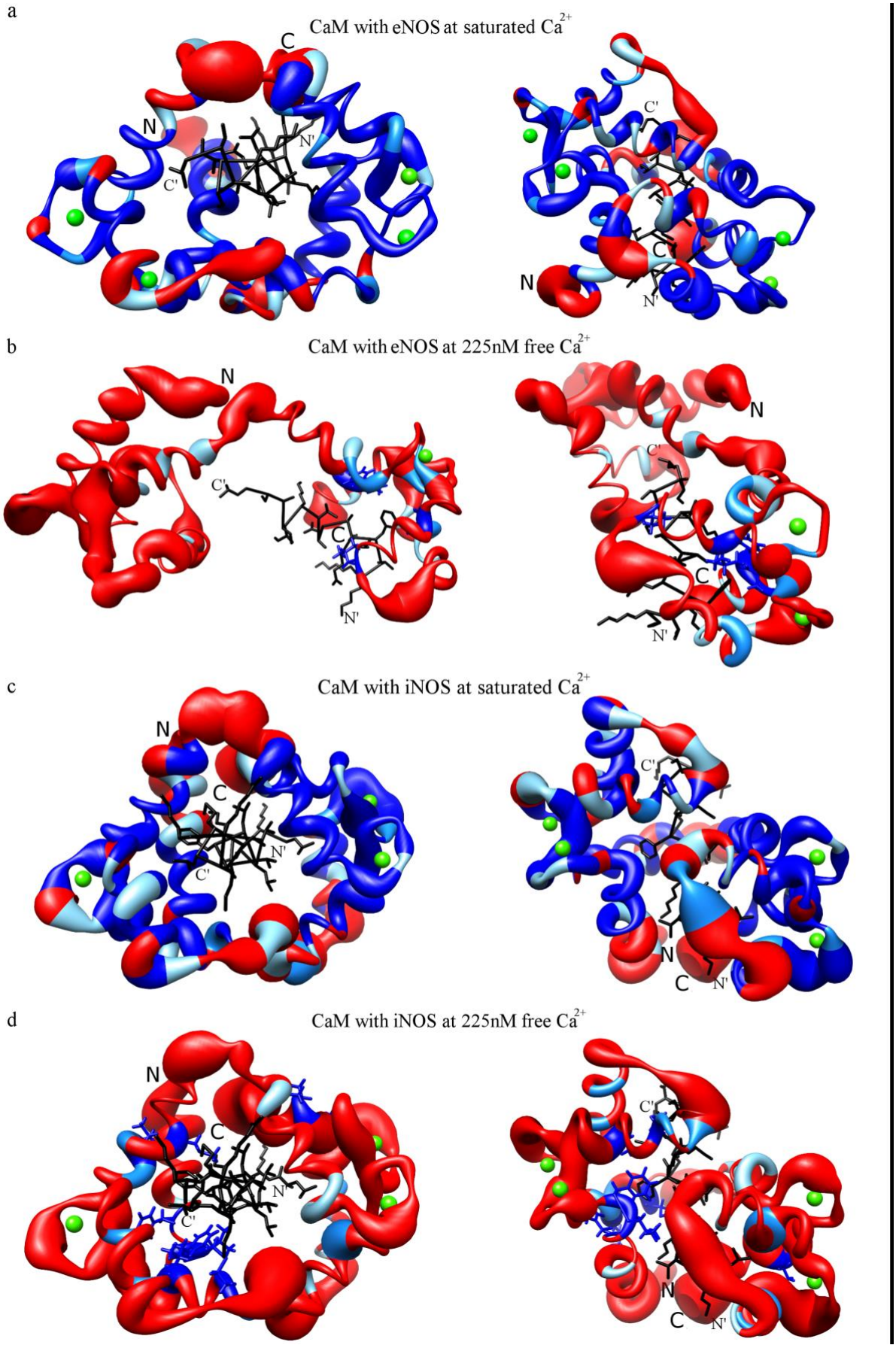
a
CaM with eNOS at saturated Ca2+
C
N
N'
C'
C'
C
N
N'
b
CaM with eNOS at 225nM free Ca2+
N
C'
C
N'
N
C'
C
N'
c
CaM with iNOS at saturated Ca2+
N
C
N'
C'
C'
N
C
N'
d
CaM with iNOS at 225nM free Ca2+
N
C
N'
C'
C'
N
C
N'

Figure 6

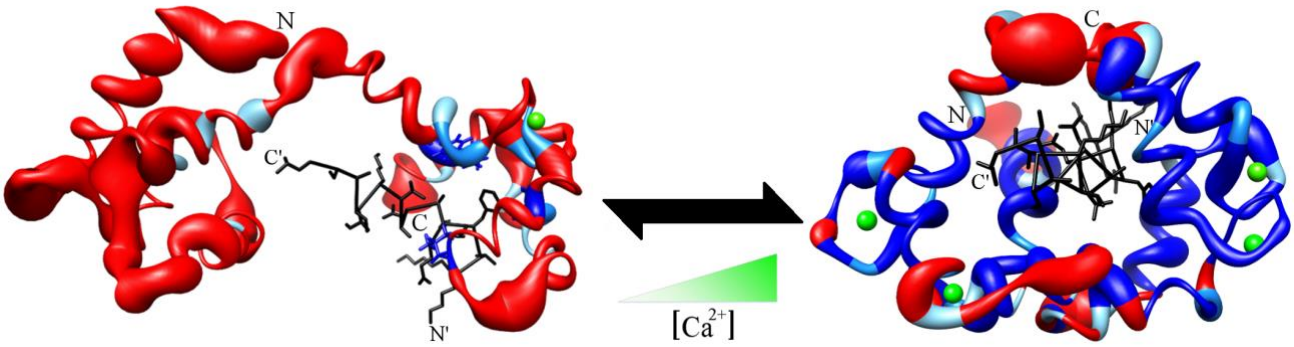

Table of Contents Figure